J Solid State Electrochem (2000) 4: 408–416

ORIGINAL PAPER

Annamalai Senthil Kumar · K. Chandrasekara Pillai

Studies of electrochemical behaviour of RuO_2-PVC film electrodes: dependence on oxide preparation temperature

Received: 12 August 1997 / Accepted: 18 October 1999

Abstract Ruthenium dioxide electrodes, prepared on a Pt substrate using coatings of PVC-RuO_2 mixed in THF (designated as RuO_2-PVC film electrode) have been studied for their redox behaviour in 1 M NaOH using variable scan cyclic voltammetry. The various redox transitions in the oxidation state of the central metal ion are characterized using electrochemical parameters such as peak potential, peak current, and surface charge. The effect of oxide preparation temperature, in the range 300–700 °C, on the redox characteristics has also been studied and correlated with the electrochemically active surface area (as measured using small amplitude cyclic voltammetry) and the true surface area (by the BET method).

Key words Ruthenium dioxide powder · PVC film electrodes · Surface charge · Electrochemically active surface area · BET surface area

Introduction

Ruthenium dioxide (RuO_2) is a well-known important electrochemical material that has long been in use as an electrode for catalyzing multi-electron transfer reactions like Cl_2, O_2 evolution, and organic oxidation reactions [1–3]. Recent renewed interest in RuO_2 is related to its high power density capacity, which has extended its use in electrochemical capacitors [4]. Conventionally, RuO_2 electrodes have been prepared by thermal decomposition of $RuCl_3 \cdot xH_2O$ on suitable substrates like Ti or Pt at temperatures in the range 300–700 °C [1]. Several parameters such as the method of pretreatment, the solvents used as vehicles for coating the $RuCl_3$ salt, the way in which the coatings have been applied (whether successive or one-time coating), the mode of heating, etc., have been found to exert considerable effect on the stability and nature of the RuO_2 coating formed on the substrate materials [1, 5]. Fox example, use of HCl as solvent has been reported to lead to cracked films [1], while with organic solvents like isopropanol, compact films have been obtained with no cracks [5]. Various methods have therefore been attempted in the past in order to prepare RuO_2 electrodes by alternate routes. Thus, Teflon-bonded RuO_2 electrodes [6, 7], RuO_2-modified carbon paste electrodes [8], and RuO_2-modified graphite-epoxy composite electrodes [9] have all been prepared and used in various electrochemical studies. Recently, we have fabricated PVC-bonded RuO_2 composite electrodes on Pt substrates by a much simpler method using tetrahydrofuran (THF) and used it for glucose oxidation [10]. In this paper, we describe the electrochemical behavior of these RuO_2-PVC film electrodes in 1 M NaOH. The main object of the present work was to examine the effect of oxide preparation temperature on the electrochemical behavior of these electrodes. Our results suggest that the variation in interfacial charge transfer behavior of the oxide electrodes can be directly correlated to the changes in electrochemically active surface area or BET surface area arising from the use of to different preparation temperatures.

A.S. Kumar · K. Chandrasekara Pillai (✉)
Department of Physical Chemistry,
University of Madras,
Guindy Campus, Madras 600 025, India
e-mail: kchandra@unimad.ernet.in
Fax: +91 44 2352870

Experimental

Materials

$RuCl_3 \cdot xH_2O$ (Arora Matthey) and PVC (Fluka) were used without further purification. The solvent THF of Analar grade was distilled three times in the presence of sodium wire.

Electrochemical instrumentation

Cyclic voltammetry (CV) was performed with a Wenking potentiostat (model ST 72), Wenking scan generator (model VSG 83), and Graphtec XY recorder (model WX 2300). Rotating disc

electrode (RDE) experiments were performed using Pine instrument (USA). A large area platinum plate was used as a counter electrode and an SCE with a luggin capillary as a reference electrode. N_2 gas was used for deaerating the experimental solution.

Preparation of RuO_2 powders

RuO_2 powders were prepared by the usual procedure [11]. Briefly, $RuCl_3 \cdot xH_2O$ dried at 100 °C for 1 h was heated in the presence of O_2 for 6 h in a muffle furnace at the pre-set preparation temperature (300–700 °C). The samples were taken out, crushed, and finally heated at the same temperature for 6 h. The powders were then repeatedly washed with charcoal-treated double-distilled water until the solution gave a negative test for Cl^- with Ag^+. Washed samples were dried at 110 °C for 12 h and stored in desiccator until use.

Preparation of RuO_2-PVC film electrodes

RuO_2 and PVC (4:1 wt%) were mixed well in a minimum quantity of THF. The RuO_2-PVC paste was then coated onto the surface of a platinum wire electrode, and air dried at room temperature for 48 h. In order to obtain well-bonded, mechanically stable coatings, it was essential to use freshly distilled THF and to polish and clean the surface of the substrate Pt electrode prior to coating the films. Therefore, in this study the Pt electrode surface was polished gently with emery paper (no. 800, Carborundum Universal, India), cleaned with 20% HCl for 20 min, washed, and dried. Poor adhesion of the coating to the Pt substrate was easily detected by observing the increased asymmetry in the voltammetric peaks or tilting of the voltammogram with respect to the potential axis. The effective loading of oxide on each electrode was around 40 mg cm^{-2} of geometric area.

Electrode surface pretreatment

All freshly prepared RuO_2-PVC film electrodes were initially preconditioned. Preconditioning consisted of cycling the electrode potential in the region −1100 to +450 mV (SCE) in 1 M NaOH at a potential scan rate (v) of 20 mV s^{-1} several times until the voltammograms, which initially showed a systematic current increase, remained constant. It normally took 1–2 h to achieve this result.

In order to commence the voltammetric experiments starting with a similar, reproducible electrode surface, the RuO_2 composite electrode was pretreated once at the start of every day. Pretreatment consisted of cycling the electrode potential five times between the potentials −1100 to +450 mV in 1 M NaOH at $v = 20$ mV s^{-1}. The most reproducible peak potentials were obtained by the above pretreatment method.

Results and discussion

Electrochemistry of RuO_2(700 °C)-PVC film electrode in 1 M NaOH

Initially, cyclic voltammetric studies were carried out with a RuO_2-PVC composite electrode made out of powders prepared at 700 °C. Typical CVs in 1 M NaOH solution are shown in Fig. 1 for various scanning rates. The voltammograms have been recorded by scanning the potential in anodic direction starting from −1100 mV (SCE) and reversing the scan at +450 mV to record the negative going cycle. There appears a large background current with three anodic peaks (A1, A2, and A3) at potentials −400, 0, 320 mV (SCE), respectively. Three cathodic peaks (C1, C2, and C3) appear in the negative going cycle at −360, 35, and 300 mV (SCE). The number for each peak is given in such a way that the same number for the anodic and cathodic peak makes a redox couple. The cathodic counter parts of the anodic peaks were identified by varying the switching potential in the CV. The redox pair A1/C1 shows a smaller current and broader peak compared to the redox pairs A2/C2 and A3/C3. This made the measurement of peak current (i_p) and peak potential (E_p) difficult, especially i_p values, for A1/C1.

Figure 2A indicates that, for the A3 and A2 peaks, log(current density) varies linearly with log(scan rate) with a slope 1 in the lower scan rate region, and ~0.5 at higher potential scan rates. The scan rate dependence clearly suggests that the redox processes occur as surface-confined electron transfer processes at low scan rates, and as mass transport by diffusion coupled to electron transfer processes at higher scan rates [12]. Note that the peak potentials (E_{Pa} and E_{Pc}) remain scan rate independent in the lower scan rate regions, but shift to higher polarizations as the scan rate increases (beyond 20 mV s^{-1} for A3/C3, and beyond 40 mV s^{-1} for A2/C2), as shown in Fig. 2B. It is observed that the peak current ratios of cathodic and anodic peaks are approximately one for the A3/C3 and A2/C2 redox pairs.

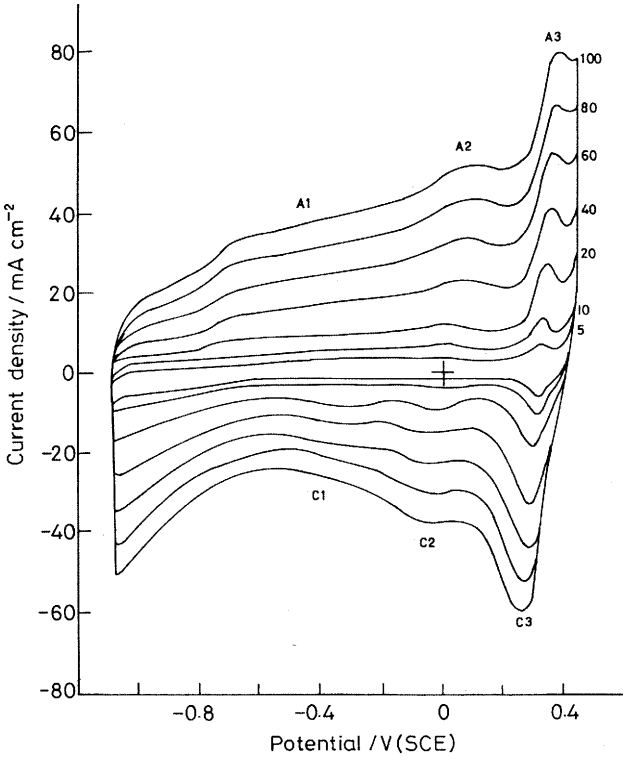

Fig. 1 Cyclic voltammograms of RuO_2(700 °C)-PVC film electrode in 1 M NaOH in the potential region −1.10 to +0.45 V (SCE) at various scan rates

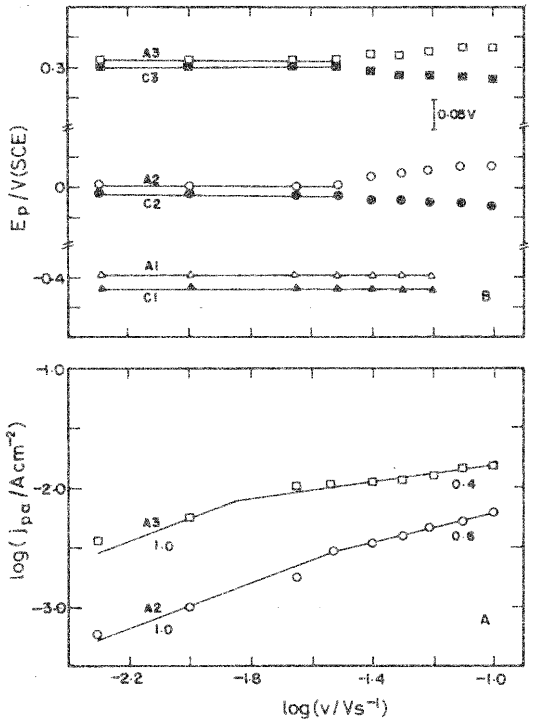

Fig. 2 A Variation of log(anodic peak current density) with log(scan rate); **B** variation of peak potential with log(scan rate) for RuO_2(700 °C)-PVC film electrode in 1 M NaOH

More importantly, the peak current and their potentials are not dependent upon electrode rotation. The $E_{1/2}$ values, obtained as $(E_{Pa} + E_{Pc})/2$, are −380, 18, and 310 (SCE) for the redox couples A1/C1, A2/C2, and A3/C3 in 1 M NaOH. These values agree well with those reported for RuO_2 electrodes prepared by a high-temperature decomposition method [13, 14]. Thus the peaks A1/C1, A2/C2, and A3/C3 can be identified with the surface redox transitions Ru(IV)/Ru(III), Ru(VI)/Ru(IV), and Ru(VII)/Ru(VI), respectively.

Effect of solution pH

To establish the stoichiometry of the redox reactions, CV measurements were extended to phosphate buffer of pH 7, acetate buffer of pH 4.6, and 1 M H_2SO_4 solutions. The important observations made with these results are the following: (1) unlike in 1 M NaOH, only two redox transitions, A1/C1 and A2/C2, are present in these solutions in the potential region between the H_2 and O_2 evolution reactions, as observed previously for thermally prepared RuO_2 electrodes [13, 15], (2) similar to that in 1 M NaOH, the anodic peak currents in these solutions vary with the scan rate as in Fig. 2A; and also (3) the voltammograms are independent of electrode rotation.

The $E_{1/2}$ is plotted against pH in Fig. 3. A slope of −75 mV per unit increase in pH is obtained for both A1/C1 and A2/C2 redox pairs of the RuO_2-PVC composite electrodes in the wide pH range 1–14, as noticed by others for thermally prepared RuO_2 electrodes [13, 14]. The non-Nernstian values indicate that the redox reactions could occur by involving non-integral values for charge and hydroxide ion. Hence the peaks can be identified with the following redox surface processes:

A1/C1:

$$(\text{—O—})_2\text{Ru}^{\text{III}}\text{O}^-(\text{OH})_3 + 1.25\text{OH}^- \rightleftharpoons (\text{—O—})_2\text{Ru}^{\text{IV}}\text{O}^-(\text{OH})_{1.25}^{-0.25}(\text{H}_2\text{O})_{1.75} + 1.25\text{H}_2\text{O} + \text{e}^- \quad (1)$$

A2/C2:

$$(\text{—O—})_2\text{Ru}^{\text{IV}}\text{O}^-(\text{OH})_{1.25}^{-0.25}(\text{H}_2\text{O})_{1.75} + 2.5\text{OH}^- \rightleftharpoons (\text{—O—})_2\text{Ru}^{\text{VI}}\text{O}_{1.75}^{-1.75}(\text{OH})_{2.25} + 2.5\text{H}_2\text{O} + 2\text{e}^- \quad (2)$$

The fractional charge values and non-stiochiometric surface compounds indicate the participation by polymeric or inter-linked surface species [14]. In the above scheme RuO_2 is represented as **1** by taking into account

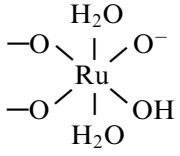

1

the hydration of the surface oxyhydroxide groups of RuO_2 particles in NaOH [14, 16]. As the redox pair A3/C3 is present only in solutions of pH exceeding 13 [14, 15, 17], with dE_p/dpH around −80 mV [14, 17], A3/C3 corresponds to the following redox reaction, as suggested by Lyons and Burke [14]:

A3/C3:

$$(\text{—O—})_2\text{Ru}^{\text{VI}}\text{O}_{1.75}^{-1.75}(\text{OH})_{2.25} + 1.25\text{OH}^- \rightleftharpoons (\text{—O—})_2\text{Ru}^{\text{VII}}\text{O}_{2.75}^{-3.00}(\text{OH})_{1.25} + 1.25\text{H}_2\text{O} + \text{e}^- \quad (3)$$

Nature of the redox processes

At higher scan rates

The $v^{1/2}$ dependence of j_{Pa} (Fig. 2A) indicates that the diffusion is coupled to the self-exchange electron transfer processes of Eq. 1–3 between the ruthenium oxidation states in RuO_2 material. The dependence on pH of the solution (Fig. 3) suggests that the ionic species OH^- in base (or H^+ in acid) is the diffusing ion. If the transport of the diffusing ion in bulk solution occurs on the voltammetric time scale, then the voltammetry should be

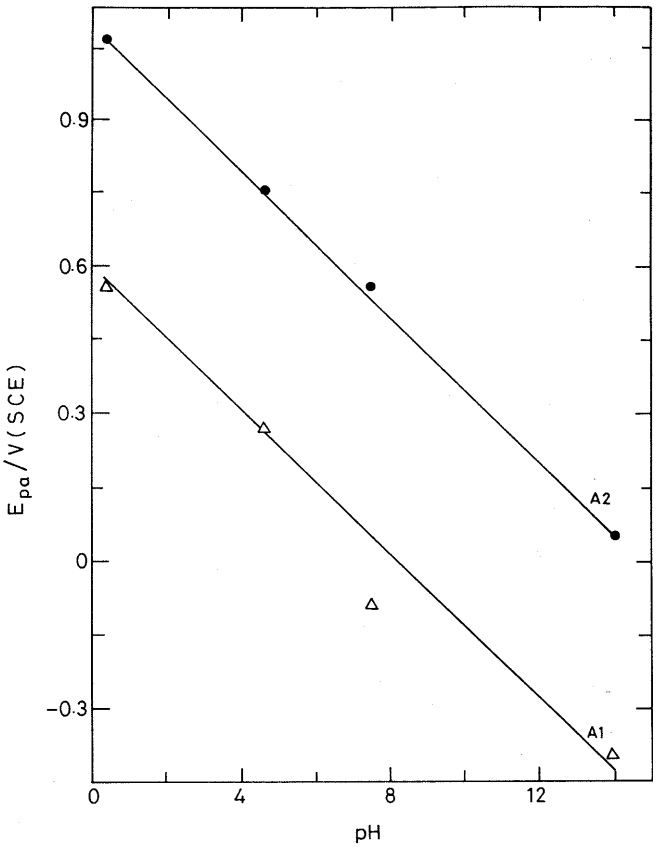

Fig. 3 Variation of anodic peak potential with solution pH for RuO_2(700 °C)-PVC film electrode

modified by stirring the solution. However, the results obtained in the present study of the electrode rotation effect demonstrate that both the peak position and peak current for all the three pairs of peaks do not depend on solution stirring speed over the wide pH range 0–14. By inference, the data are then explicable in terms of diffusion of electrolyte ion, i.e. OH^- (or H^+), occurring within the solid [18].

In order to verify further that the mass transfer of the proton in the RuO_2 solid, rather than its mass transfer in solution, controls the redox processes of Eq. 1–3, we have calculated the mass transfer parameter

$$z = (D_{ss}/D_{aq})^{1/2}\rho/[C^+]^* \quad (4)$$

proposed by Lovric et al. [19] for a solid state redox reaction accompanied by the insertion or expulsion of electrolyte ions in the solid. According to these authors, the voltammetric response is independent of the mass transfer in the solution provided that the parameter z is smaller than 0.1. In Eq. 4, D_{ss} is the diffusion coefficient of the cation C^+ in the crystal, D_{aq} is its diffusion coefficient in the solution, ρ the density of the solid compound (mol cm^{-3}), and $[C^+]^*$ the concentration of C^+ ions in the bulk of the solution (mol cm^{-3}). Taking the density of the RuO_2 solid compound as 6.27 g cm^{-3} [20], and a molar mass of 133.08, this gives $\rho = 4.712 \times 10^{-2}$ mol cm^{-3}. With $D_{ss} = 5.0 \times 10^{-18}$ m^2 s^{-1}, from the published data of Weston and Steele [21], for the diffusion coefficient of H^+ in RuO_2 powders prepared at 700 °C, $D_{aq} = 3.4 \times 10^{-9}$ m^2 s^{-1} for the diffusion coefficient of H^+ at 25 °C [20], and $[H^+]^* = 2 \times 10^{-3}$ mol cm^{-3}, z is calculated to be 9.0×10^{-4} in 1 M H_2SO_4. The small value for z shows that the mass transfer of H^+ in solution is negligible in the redox reactions (Eq. 1–3) of the RuO_2-PVC film electrode.

It must be mentioned here that the voltammograms recorded between 0 and 1450 mV (RHE) continuously run for over 3 h showed only marginal increase (~5%) in voltammetric current. Similar behavior has been observed, for instance, by Doblhofer et al. [22] and Jang et al. [23] for thermally prepared RuO_2 electrodes. They explain their findings in terms of the high structural stability of RuO_2 powders [22], a gradual "opening-up" of the oxide pore structure as a result of voltammetric cycling (time effect) [23], etc. It has been argued [22] that if the diffusion process into the solid were to be volume diffusion, the oxidation state of the bulk ruthenium had to change by several steps more or less reversibly; this process would then be associated with lattice dilation and contraction, contrary to the experimental observation [22]. Thus proton diffusion into the solid RuO_2 is suggested to take place presumably along grain boundaries, micropores, and microcracks. Note that from the electrochemical studies alone it is hard to distinguish between volume diffusion and grain boundary diffusion mechanisms. Direct monitoring, by in situ techniques like XRD [24], atomic force microscopy (AFM) [25], etc., of the dimensional changes of RuO_2 material occurring during electrochemical processes may give some insight to help the basic understanding of proton diffusional pathways. A detailed investigation of these aspects is in progress.

At lower scan rates

The results at low scan rates, namely that the CVs of RuO_2 have symmetric peak shapes and nearly equal heights of oxidation and reduction peaks, the oxidation peak heights increase linearly with v (Fig. 2A), the peak potentials are independent of v (Fig. 2B), and the CVs are not affected by electrode rotation, are all characteristics of reversible surface reactions [12]. It may be noticed that even in the experimental studies of some solid state redox reactions accompanied by the insertion or expulsion of electrolyte ions in the solid, it has been seen that some reactions are initially surface confined [26, 27] whereas others advance throughout the crystal from the very beginning [28]. The peak separation (E_{pa}–E_{pc}), however, is not equal to zero, for either of the three redox pairs of RuO_2-PVC film electrode (Fig. 2B), indicating deviation from ideal behavior for surface-confined species. This could be caused by the site-site interactions (thermodynamic effect), slow charge transfer (kinetic effect), or large uncompensated electrolyte

resistance effects [29–31]. In a similar way, the potential of full width at the half maximum (E_{fwhm}) is much different from the theoretical value of $90/n$ (where n = number of electrons transferred per electroactive site) predicted for ideal reversible redox centers [29, 30]. E_{fwhm} is around 50 mV for A3/C3 and it is 150 mV for A2/C2 at slow potential scan rates, typically 5 mV s^{-1}. The presence of interaction effects alters the peak half-width and equality of peak currents [12, 29, 30]. The interaction term r of the redox pairs associated with the RuO_2-PVC film electrode is estimated from the surface activity relationship for interacting sites [29–31].

The i_p is related to r as:

$$i_p = n^2F^2A\Gamma_t v/RT[4 - 2r\Gamma_t] \quad (5)$$

Since $q_t = nFA\Gamma_t$, then:

$$i_p = nFq_t v/RT[4 - 2r\Gamma_t] \quad (6)$$

where A is the geometric area of the electrode in cm^{-2}, q_t is the total surface charge, and Γ_t is the total surface concentration of redox sites. The other symbols R, T, and F have their usual significance. The ratio of the i_p-v slope (in the scan rate region 0–20 mV s^{-1} for A3, and 0–40 mV s^{-1} for A2) to the charge under the peak gives a value of $nF/RT(4–2r\Gamma_t)$ according to Eq. 6. For the anodic peak A3 with $n = 1$, since the redox transition corresponds to Ru(VI)/Ru(VII) (see reaction 3), and $\Gamma_t = 2.37 \times 10^{-7}$ mol cm^{-2} (estimated from the area under the peak recorded at low v, typically 5 mV s^{-1}), r is calculated to be 7.24×10^6 cm^2 mol^{-1}. For peak A2, r is -1.2576×10^7 cm^2 mol^{-1}, corresponding to $\Gamma_t = 2.376 \times 10^{-7}$ mol cm^{-2} and $n = 2$ [Ru(IV)/Ru(VI) transition, see reaction 2]. The positive r for A3 indicates that attractive interaction exists amongst the redox sites of A3/C3 in the surface layer, whereas repulsion is predominant within the redox centers of the A2/C2 redox couple, since r is negative for the A2 peak. The observation that peak A2 is quite broad and the charge possessed by this peak (6.21 mC) is less than double the charge of peak A3 (2×5.0 mC), in spite of the fact that A2 involves two electrons while A3 involves one electron, is probably due to the negative interaction associated with A2. However, there are other possible explanations. These include a following chemical reaction accompanying the Ru(IV)/Ru(VI) electron transfer step, as discussed by Lam et al. [32].

Effect of oxide preparation temperature on the electrochemical behavior of the RuO_2-PVC film electrode

Electrodes were fabricated with RuO_2 powders prepared at various temperatures (300–700 °C). Figure 4 shows the CV recorded at 20 mV s^{-1} for RuO_2 electrodes for five different temperatures (300, 400, 500, 600, and 700 °C). It shows that the electrochemistry of RuO_2 electrodes is remarkably dependent on the oxide preparation temperature. Increased preparation temperature decreased the current density. Uniform trends are observed for background current, peak shape, and peak intensity as the oxide preparation temperature is varied. At 300 °C the background current is quite high, but at the same time there is a reduction in surface peak shape and peak intensities. Furthermore, the surface redox peaks become broader. These result in greater difficulties in measuring the surface peak intensities for samples of lower temperatures. In order to quantitatively compare the electrochemical behavior of the electrodes with oxide preparation temperature, the electrochemical charge that is sustained during the polarization, both cathodic and anodic, has been calculated for various samples.

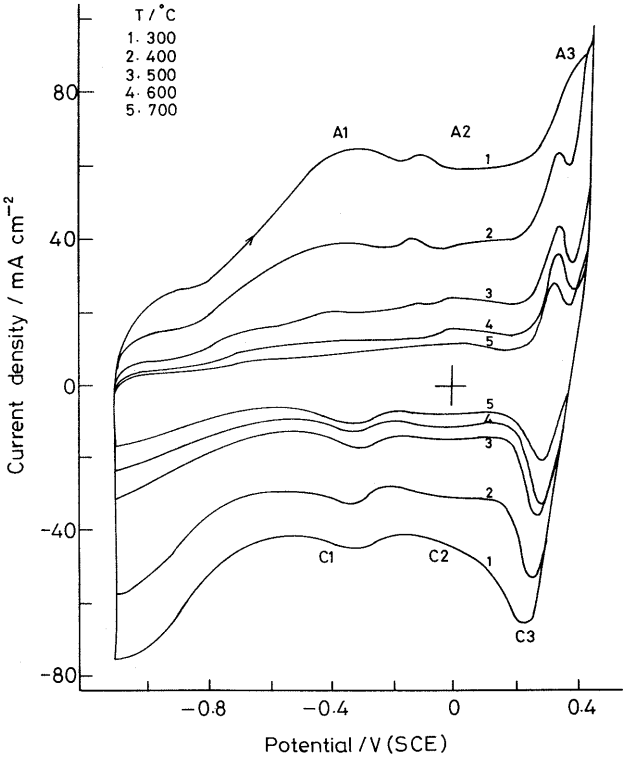

Fig. 4 CV of RuO_2-PVC film electrode fabricated using RuO_2 powders prepared at various temperatures. Electrolyte: 1 M NaOH; potential region: −1.10 to +0.45 V (SCE); scan rate = 20 mV s^{-1}

The total charge density calculated based on the apparent electrode area, anodic (Q_a) and cathodic (Q_c), were obtained from the area under the cyclic voltammograms recorded in the potential region −1100 to 450 mV (SCE) at various scan rates. A Planimeter (Planix, Japan) was used for calculating the integral area under the voltammograms. Figure 5 shows these plotted against the scan rate for samples at various temperatures. It is obvious that both Q_a and Q_c increase with the decrease in the oxide preparation temperature. This behavior could be the result of enhanced electron transfer rates (kinetic effect) or, alternatively, the result of an increase in the electrochemically active surface area (geometric effect).

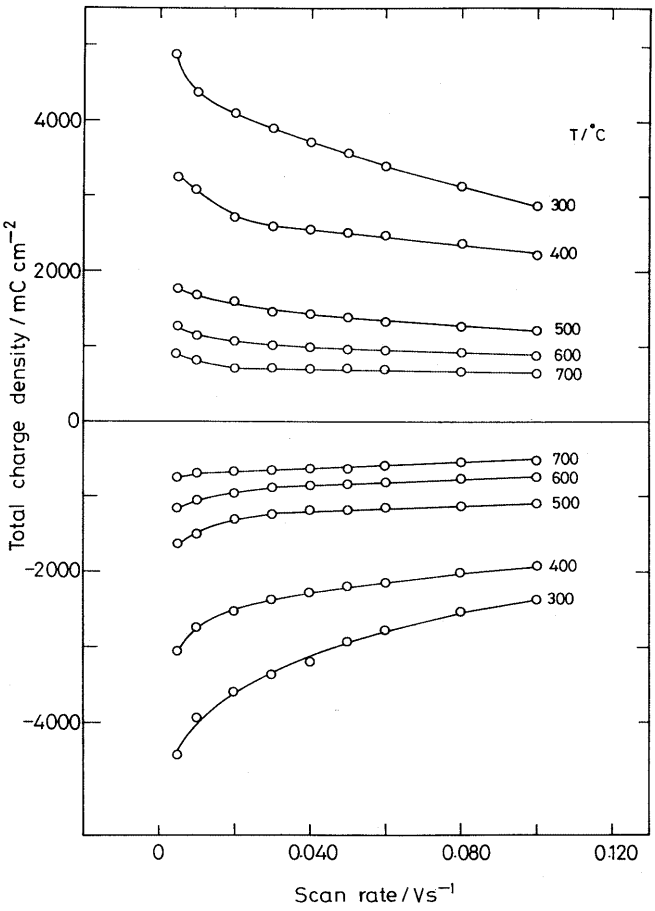

Fig. 5 Variation of total charge density with scan rate for RuO_2-PVC film electrode (at various T/°C) in 1 M NaOH

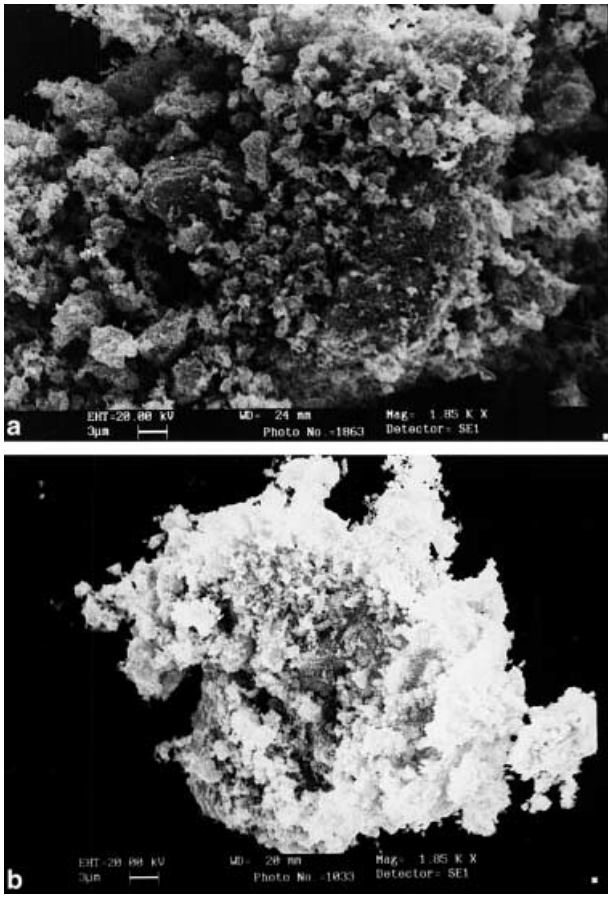

Fig. 6A,B Electron micrographs of RuO_2 powder samples (Leica stereoscan 440, cambridge instrument): **A** RuO_2 (700 °C); **B** RuO_2 (300 °C)

Figure 5 also shows that both Q_a and Q_c decrease as the scan rate is increased for all the samples; however, the rate of decrease is a function of the oxide preparation temperature. For example, the 300 °C sample shows higher variation in Q_a and Q_c initially, but at scan rates > 20 mV s^{-1} there is relatively a small change in Q values for all conditions. For the 700 °C sample the surface charge values are almost constant in the entire scan rate region investigated. According to Trasatti's formalism [33], for a given specific sample the surface charge variation with scan rate arises due to the existence of both inner and outer active surface sites coupled with the associated difficulties for proton access to the inner region of the surface (pores, cracks, and grain boundaries). The lack of appreciable dependence of Q on v for the 700 °C sample suggests the existence of negligible inner active surface sites with this electrode. Indeed, the BET surface area and the scanning electron microscope measurements support this conclusion.

The pore specific volumes obtained from the BET surface area measurements are listed in Table 1 for the various RuO_2 powder samples. The fact that the pore specific volume is smaller for the 700 °C RuO_2 sample, compared to those for other samples, clearly suggests that the former material possess much fewer micropores than the other samples; therefore, it contains fewer inner active surface sites. Figure 6 shows some representative

Table 1 BET Surface area results of RuO_2 powder samples, double layer capacity (C_{edl}) and electrochemically active surface area (A_e) of RuO_2-PVC film electrodes as a function of oxide preparation temperature

Oxide preparation temperature (°C)	BET surface area results		Electrochemical results	
	True surface area (10^3 cm^2)	Pore specific volume (10^3 cm^3 g^{-1})	C_{edl} (mF cm^{-2})	A_e (10^3 cm^2)
300	2.824	21.290	1139.9	2.155
400	1.376	10.790	791.7	1.408
500	1.094	8.543	450.0	0.841
600	1.276	9.547	319.3	0.582
700	0.798	6.151	214.6	0.415

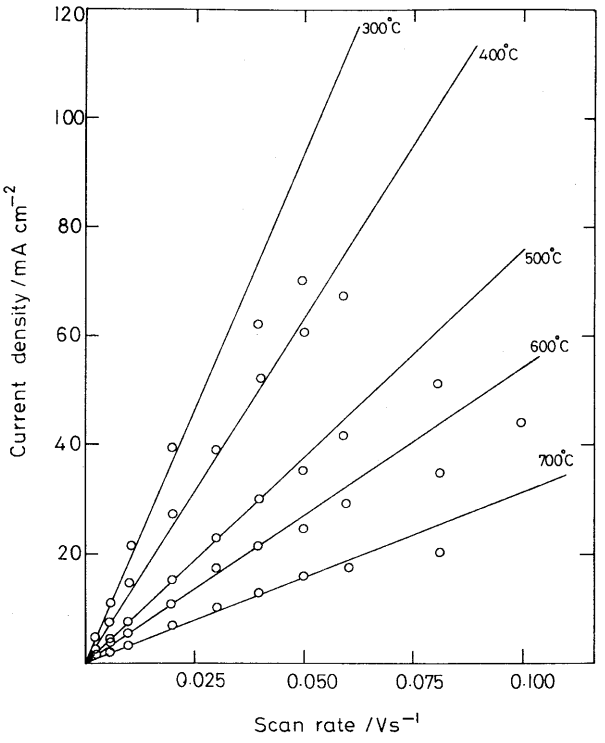

Fig. 7 Capacitative charging current density versus scan rate in 1 M NaOH for RuO_2-PVC film electrodes of various oxide preparation temperatures

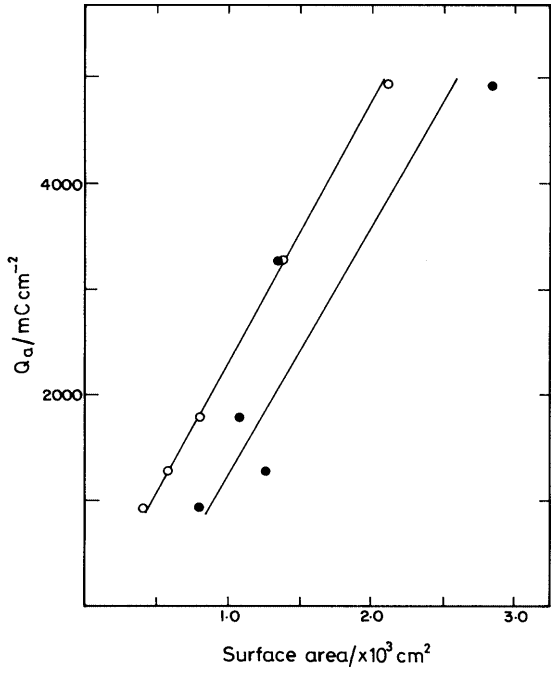

Fig. 8 Surface charge density as a function of surface area for RuO_2-PVC film electrodes: (–○–○–) electrochemically active surface area; (–●–●–) BET surface area

micrographs of RuO_2 powders (Leica Stereoscan, Cambridge Instruments). As shown in Fig. 6A, the 700 °C RuO_2 sample contains large crystallites along with numerous agglomerates possessing less pores and grain boundaries, compared to the SEM of the 300 °C RuO_2 sample (Fig. 6B), which is characterized by microscopically homogeneous spongy-like porous material.

Electrochemically active surface area measurements

Using the small amplitude CV technique, a crude estimate of the electrochemically active surface area (A_e) of each film electrode was obtained from double-layer charging curves in 1 M NaOH solution. This method has been frequently used for the estimation of the double-layer capacity of large surface area and porous electrodes [34, 35], including ruthenium-based mixed oxides [36, 37]. Voltammograms were recorded in 1 M NaOH at various scan rates in a narrow potential region of 0–150 mV (SCE), so that the *i-E* curves showed almost a flat current plateau with no maxima. It must, however, be remembered that there is some residual faradaic current present in this potential range as well, which tends to contaminate the A_e results to some extent, since with RuO_2 electrodes there is a large faradaic current at all potentials from −1100 to +450 mV (SCE) (arising by the electrochemical reactions 1–3) over and above a huge non-faradaic charging current [4].

A plot of the charging current density (j_{cha}) measured at the middle of the potential region (where the anodic and cathodic currents are equal in magnitude) versus scan rate is linear for all the five samples, as shown in Fig. 7. Deviations from linearity are observed at high scan rates; these deviations become more pronounced for samples which are prepared at lower temperature. The slope of the j_{cha}-v plots, under the limiting condition $v \rightarrow 0$, is used to calculate the double layer capacitance (C_{edl}) of the electrode, and the values are given in Table 1:

$$C_{edl} = \frac{j_{cha}}{v} F \text{ cm}^{-2} \quad (7)$$

Once C_{edl} is known, A_e is calculated as in the previous studies [34, 35, 37], by considering the literature value of 70 μF cm^{-2} for the microscopic area of RuO_2 colloidal particles [38]. Similar to that noticed earlier for thermally prepared RuO_2 electrodes [39], the calculated electrochemically active surface area of the RuO_2-PVC film electrodes is found to increase with a decrease in the oxide preparation temperature (see Table 1), as does the surface charge density (see Fig. 5). A direct comparison of Q_a against the corresponding A_e is illustrated in Fig. 8. Also shown on this diagram is the variation of surface charge with BET surface area of the RuO_2 powder. The charge density values at the lowest v have been used in the comparisons, since according to Trasatti's formalism the charge density at low v is a measure of the total active surface sites [33]. Figure 8 shows that the electrochemically active surface area is smaller than

the BET surface area for most of the samples. This may be because while the BET method gives the total surface area, the small amplitude CV technique probably gives a better estimate of the electrochemically accessible area, since liquid phase adsorption is involved. It is also possible that the value of 70 μF cm^{-2} assumed for the microscopic area of RuO_2 particles [38] in the A_e calculation is approximate [34]. It is evident from Fig. 8 that the surface charge density varies almost linearly both with the electrochemically active surface area and the BET surface area. The near linear variation between Q_a and the surface area (electrochemically active or BET) forms direct evidence to show that the electrochemical charge of a RuO_2-PVC composite electrode primarily depends on the surface area of the oxides, and other factors, notably the kinetic effect, appear to be secondary in influencing the interfacial electron transfer process associated with these electrodes in alkaline solutions. Probably this property makes RuO_2 more suitable as electrochemical capacitors [4].

The present electrodes were also examined for their stability. A periodic check of these electrodes was made by repeating the potential cycling between −1100 to 450 mV (SCE). The voltammogram did not show any variation in shape of the curve and no difference was observed in voltammograms recorded on different days. Thus, our studies indicate that the electrode preparation method using PVC as a binder forms an alternative to fabricate RuO_2 electrodes, with behavior similar to that of thermally prepared electrodes. Moreover, PVC-based RuO_2 electrodes offer several advantages over their thermally prepared counterparts. Firstly, following the PVC method, higher amounts of RuO_2 can be used for electrode fabrication, which are more desirable for electrocatalytic applications [3]. Secondly, Cl^- free-RuO_2 electrodes can be fabricated by repeatedly washing the RuO_2 powder samples prior to electrode preparation. Finally, the common problem, that Ti or Pt support does not permit preparation at a higher temperature than 500 °C owing to interphase swelling and the formation of a fragile overlayer [1, 40], is avoided in the present PVC-based method. Besides, the use of higher loading amounts of RuO_2 (80%) reduces the resistance effects arising from the PVC binder. It must, however, be mentioned that while the present PVC-based method allows preparation of electrodes with utmost ease, its use in preparation of large surface area electrodes is not established. In this respect the PVC-based preparation method appears to possess no better advantage than the other preparation methods like Teflon-bonded [6, 7], CPE [8], or graphite epoxy electrodes [9]. In general, the distinct advantage associated with making electrodes from RuO_2 powders, compared to the thermally prepared RuO_2 electrodes, is that the RuO_2 powders can be studied for their interfacial properties by the well-founded potentiometric acid-base titration technique [16] and the results can be straightforwardly correlated with electrode kinetic studies. Work is currently in progress in this direction.

Conclusions

The RuO_2-PVC film electrodes, prepared using RuO_2 powder with PVC as a binder, show CV behavior similar to those reported earlier for thermally prepared RuO_2 electrodes. A direct correlation has been noticed with RuO_2-PVC film electrodes between their surface charge and the electrochemically active or BET surface area, as observed previously for thermally prepared RuO_2 electrodes.

Acknowledgements We gratefully acknowledge the financial support of the CSIR, New Delhi, India. We thank Prof. F. Scholz for providing us with a pre-print of ref. [19].

References

1. Trasatti S, Lodi G (1981) Properties of conductive transition metal oxides with rutile type structure. In: Trasatti S (ed) Electrodes of conductive metallic oxides, part A. Elsevier, Amsterdam, pp 301–358
2. Trasatti S (1984) Electrochim Acta 29: 1503
3. Lyons MEG (1994) Analyst 119: 805
4. Zheng JP, Jow TR (1995) J Electrochem Soc 142: L6
5. Lodi G, Bighi C, De Asmundis C (1976) Mater Chem 1: 177
6. O'Sullivan EJM, White R (1989) J Electrochem Soc 136: 2576
7. Shieh DT, Hwang JB (1995) J Electroanal Chem 391: 177
8. Lyons MEG, Fitzgerald CA (1994) Analyst 119: 855
9. Leech D, Wang J, Smyth MR (1990) Analyst 115: 1447
10. Dharuman V, Chandrasekara Pillai K (1997) Indian J Chem Technol 4: 25
11. Aridizzone S, Siviglia P, Trasatti S (1981) J Electroanal Chem 122: 395
12. Bard AJ, Faulkner LR (1980) Electrochemical methods. Wiley, New York
13. Burke LD, Murphy OJ (1980) J Electroanal Chem 109: 199
14. Lyons MEG, Burke LD (1983) J Chem Soc Faraday Trans 1 83: 299
15. Burke LD, Healy JF (1981) J Electroanal Chem 124: 327
16. Furlong DN, Yates DE, Healy TW (1981) Fundamental properties of the oxide/aqueous solution interface. In: Trasatti S (ed) Electrodes of conductive metallic oxides, part B. Elsevier, Amsterdam, pp 367–432
17. Dharuman V, Chandrasekara Pillai K (1999) Bull Electrochem 15: 476
18. Scholz F, Meyer B (1998) Voltammetry of solid microparticles immobilized on electrode surfaces. In: Bard AJ, Rubinstein I (eds) Electroanalytical chemistry, vol 20. Dekker, NewYork, pp 1–86
19. Lovric M, Hermes M, Scholz F (1998) J Solid State Electrochem 2: 401
20. Weast RC (1989) CRC handbook of chemistry and physics, 70th edn. CRC, Boca Raton, p F-49
21. Weston JE, Steele BCH (1980) J Appl Electrochem 10: 49
22. Doblhofer K, Metikos M, Ogumi Z, Gerischer H (1978) Ber Bungsenges Phys Chem 82: 1046
23. Jang GW, Tsai EW, Rajeshwar K (1989) J Electroanal Chem 263: 383
24. Chianelli RR, Seanlon JC, Rao BML (1978) J Electrochem Soc 125: 1563
25. Alliata D, Haring P, Haas O, Kötz R, Siegenthalar H (1999) Electrochem Commun 1: 5
26. Bond AM, Marken F (1994) J Electroanal Chem 372: 125
27. Bond AM, Cooper JB, Marken F, Way DM (1995) J Electroanal Chem 396: 407

28. Lovric M, Scholz F (1997) J Solid State Electrochem 1: 108
29. Brown AP, Anson FC (1967) Anal Chem 49: 1589
30. Smith DF, Willman K, Kuo K, Murray RW (1979) J Electroanal Chem 95: 217
31. Ilangovan G, Chandrasekara Pillai K (1997) Langmuir 13: 566
32. Lam KW, Johnson KE, Lee DG (1978) J Electrochem Soc 125: 1069
33. Ardizzone S, Fregonara G, Trasatti S (1990) Electrochim Acta 35: 283
34. Trasatti S, Petrii OA (1991) Pure Appl Chem 63: 711
35. Marson B, Fradette N, Beaudoin G (1992) J Electrochem Soc 139: 1889
36. Tilak BV, Rader CG, Rangarajan SK (1977) J Electrochem Soc 124: 1879
37. Yeo RS, Orehotsky J, Visscher W, Srinivasan S (1981) J Electrochem Soc 128: 1900
38. Kleijn M, Van Leeumen HP (1988) J Electroanal Chem 247: 253
39. Burke LD, Murphy OJ, O'Neil JF, Venkatesan S (1977) J Chem Soc Faraday Trans 1 73: 659
40. Galizzioli D, Tantardini F, Trasatti S (1974) J Appl Electrochem 4: 57